Geometry-Aware Distributed Kalman Filtering for Affine Formation Control under Observation Losses

Li, Zhonggang; Rajan, Raj Thilak

DOI
10.23919/FUSION52260.2023.10224101

Publication date
2023

Document Version
Final published version

Published in
2023 26th International Conference on Information Fusion, FUSION 2023

Geometry-Aware Distributed Kalman Filtering for Affine Formation Control under Observation Losses

Zhonggang Li and Raj Thilak Rajan
Signal Processing Systems, Faculty of EEMCS, Delft University of Technology, Delft, The Netherlands
{z.li-22, r.t.rajan}@tudelft.nl

***Abstract*—Affine formation control of multiagent systems has recently received increasing attention in various applications. The distributed control of these agents, under single integrator dynamics, relies on the observations of relative positions of the neighboring agents, which when unavailable is detrimental to the mission. In this paper, we propose an adaptive fusion estimator of the relative positions under intermittent and consecutive observation loss settings. A relative affine localization (RAL) solution is developed by exploiting the geometry of affine formation, which is then embedded into a distributed relative Kalman filtering (RKF) framework, leading to the geometry-aware relative Kalman filter (GA-RKF). We show through simulations that the GA-RKF exhibits enhanced robustness to both intermittent and consecutive observation losses, as compared to RAL and existing state-of-art methods.**

***Index Terms*—formation control, distributed Kalman filter, multiagent systems, sensor fusion**

I. Introduction

Distributed formation control of multiagent systems plays a vital role in various fields, such as cooperative object transport [1], [2], space interferometry [3], [4], and underwater sensing [5], [6], to name a few. Recently, there has been a variety of formation control solutions based on the displacement of agents [7], inter-agent distances [8], or bearings [9]. In particular, a stress-based framework for affine formation control has been actively researched from a static formation control [10] to a dynamic formation control [11]. By using a leader-follower strategy, maneuvering formations can be achieved by controlling a small number of agents, whereas the other agents in this framework can be autonomously steered into the desired locations by observing relative positions with respect to neighboring agents. One of the classical paradigms in Bayesian information fusion is the Kalman filtering, where the state-space equations, comprising of the dynamic and observation models of the states are combined to estimate the unknown parameters in the minimum variance sense [12]. This framework (to some extent) is robust against intermittent observation losses as estimations can still be achieved by the dynamic model in the presence of observation losses [13], [14]. In general, Kalman filters are well suited for linear systems with or without observation loses [15], [16], and for non-linear systems, variants of the Kalman filter or other solutions have been proposed e.g., neural network-based approaches [17].

More recently, intermittent observation (or packet losses) have been addressed in the formation control community, predominantly by approximating the dynamic behavior for predictions using e.g., iterative learning control (ILC) [18], long short-term memory (LSTM) [19] or Kalman filters. However, existing works are limited to discussion on intermittent observation losses, in contrast to consecutive or permanent losses, which are rarely addressed [20]. This is due to the nature of Kalman filters where the uncertainty accumulates in the absence of observation correction, and subsequently the posterior covariance typically converges to infinity. In affine formation control networks, the occurrence of consecutive observation losses is equivalent to changing the graph connectivity of agents which may lead to suboptimal formation convergence or even instability. As such, an alternative estimation w.r.t these relative positions is crucial in this challenging scenario.

In this work, we propose adaptive fusion algorithms for affine formation control framework under observation losses In Section II, the fundamentals of affine formation control are introduced with emphasis on the importance of relative position observations. In Section III, a relative state-space model is introduced and a distributed Kalman filtering for intermittent observations as in [20] will be established. In Section IV, we explore the geometrical property of affine formations and derive a distributed linear estimator for the missing observations using available ones in the neighborhood under some constraints. Finally, we propose an adaptive fusion scheme of this estimator into the Kalman filtering framework in Section V. The solutions are evaluated under intermittent losses over a spectrum of observation availability and consecutive loss scenarios in Section VI. Conclusions and future work are highlighted in Section VII.

Notation. Vectors and matrices are represented by lowercase and uppercase boldface letters respectively such as $\mathbf{a}$ and $\mathbf{A}$. Sets and graphs are represented using calligraphic letters e.g., $\mathcal{A}$. Vectors of length N of all ones and zeros are denoted by $\mathbf{1}_N$ and $\mathbf{0}_N$ respectively. An identity matrix of size N is denoted by $\mathbf{I}_N$. The Kronecker product is $\otimes$ and a vectorization of a matrix is denoted by $\text{vec}(\cdot)$ by stacking all the columns vertically.

This work is partially funded by the European Leadership Joint Undertaking (ECSEL JU), under grant agreement No. 876019, the ADACORSA project - "Airborne Data Collection on Resilient System Architectures," and the Sensor AI Lab, under the AI Labs program of Delft University of Technology.

II. Fundamentals of Affine Formation Control

Consider a setup where N mobile agents are deployed in $\mathbb{R}^D$ where $N \geq D+1$. The agents and their pairwise connections are typically represented by a graph $\mathcal{G} = (\mathcal{V}, \mathcal{E})$, where the vertex (node) set $\mathcal{V} = \{1, ..., N\}$ denotes the identities of agents and the edge set $\mathcal{E} \subseteq \mathcal{V} \times \mathcal{V}$ denotes the information flow between agents. We assume an undirected graph, i.e., $(i,j) \in \mathcal{E} \Leftrightarrow (j,i) \in \mathcal{E}$, and the total number of undirected edges is denoted by M. The set of neighbors and the number of neighbors of node i are defined as $\mathcal{N}_i = \{j \in \mathcal{V} : (i,j) \in \mathcal{E}\}$ and $|\mathcal{N}_i|$ respectively.

Let $\mathbf{z}_i \in \mathbb{R}^D$ denote the position of agent i, then the *configuration* of all agents is defined as $\mathbf{z} = [\mathbf{z}_1^T, ..., \mathbf{z}_N^T]^T \in \mathbb{R}^{DN}$. Similarly, we define $\mathbf{z}^* = [\mathbf{z}_1^{*T}, ..., \mathbf{z}_N^{*T}]^T \in \mathbb{R}^{DN}$ as the *target configuration*, where $\mathbf{z}_i^* \in \mathbb{R}^D$ is the target position of agent i. Additionally, we define a generic configuration $\mathbf{p} = [\mathbf{p}_1^T, ..., \mathbf{p}_N^T]^T \in \mathbb{R}^{DN}$ called *nominal configuration* [11], which presents a general geometric pattern that agents are expected to maintain. The target configuration will be designed as a time-varying affine transformation of the nominal configuration to denote formation maneuvers in this formation control framework. A set that contains all affine transformations of the nominal configuration is called an *affine image* i.e.,

$$\mathcal{A}(\mathbf{p}) = \{\mathbf{z} \in \mathbb{R}^{DN} : \mathbf{z} = (\mathbf{I}_N \otimes \mathbf{\Theta})\mathbf{p} + \mathbf{1}_N \otimes \mathbf{t}\}, \quad (1)$$

where $\mathbf{\Theta} \in \mathbb{R}^{D \times D}$ and $\mathbf{t} \in \mathbb{R}^D$ are the transformation matrix and translation vector respectively. The time-varying target configuration has the form of

$$\mathbf{z}^*(k) = (\mathbf{I}_N \otimes \mathbf{\Theta}(k))\mathbf{p} + \mathbf{1}_N \otimes \mathbf{t}(k), \quad (2)$$

where the transformations $\mathbf{\Theta}(k) \in \mathbb{R}^{D \times D}$ and $\mathbf{t}(k) \in \mathbb{R}^D$ are varying across time instances k. This indicates a maneuvering pattern of rotation, scaling, translation, etc. based on the structure and values in $\mathbf{\Theta}(k)$ and $\mathbf{t}(k)$. Note that the nominal configuration is usually adopted as the initial target configuration, i.e., $\mathbf{p} \triangleq \mathbf{z}^*(0)$, and by definition, the target configuration $\mathbf{z}^*(k)$ is in affine image $\mathcal{A}(\mathbf{p})$ for all k. The maneuverability is typically ensured by a technique called *leader-follower* strategy in which a small set $\mathcal{V}_l$ of agents are set aside to be the *leaders* and the rest $\mathcal{V}_f = \mathcal{V} \setminus \mathcal{V}_l$ are the *followers*. The time-varying target formation is prescribed to the leaders while the followers only need to follow the leaders and stay in formation without any knowledge of the target configurations. The leaders will be left out of the scope of discussion as they typically occupy a small number of agents. An example of nominal formation is in Fig. 1.

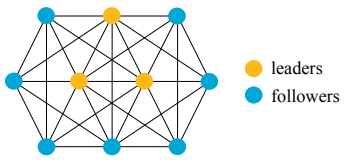

Fig. 1. An example of nominal formation in $\mathbb{R}^2$

In this work, agents will adopt single-integrator dynamics $\dot{\mathbf{z}}_i = \mathbf{u}_i$, where the control input $\mathbf{u}_i$ is taken as the velocity information $\dot{\mathbf{z}}_i$. In the discrete domain, this relation can be translated into

$$\mathbf{z}_i(k+1) = \mathbf{z}_i(k) + \Delta t \mathbf{u}_i(k) \quad (3)$$

for $i \in \mathcal{V}$, where the position of agent i is incremented by the velocity in time-interval Δt. Distributed control laws under single-integrator dynamics to track formations have been actively developed. Some control laws based on leaders' movements are shown in Table I in which all control laws rely on the observations of relative positions $\mathbf{z}_{ij} = \mathbf{z}_i - \mathbf{z}_j$ up to a translation in the neighborhood $j \in \mathcal{N}_i$. As such, the losses of these terms w.r.t. some neighbors will jeopardize the optimality of control. Note that l_{ij}s in these control laws are stress weights for edge (i,j) used to stabilize the graph.

TABLE I
Control Laws under Single-Integrator Dynamics [11]

Leaders	Control law
static	$\mathbf{u}_i = -\sum_{j \in \mathcal{N}_i} l_{ij}\mathbf{z}_{ij}$
constant velocity	$\mathbf{u}_i = -\alpha \sum_{j \in \mathcal{N}_i} l_{ij}\mathbf{z}_{ij} - \eta \int_0^t \sum_{j \in \mathcal{N}_i} l_{ij}\mathbf{z}_{ij}(\tau)d\tau$
varying velocity	$\mathbf{u}_i = -\frac{1}{\gamma_i} \sum_{j \in \mathcal{N}_i} l_{ij}(\mathbf{z}_{ij} - \dot{\mathbf{z}}_j)$

In practice, the observations are carried out by onboard sensors, which will also introduce measurement noise. Since relative localization methods abound, the modeling of the observation also differs [21]. We assume an additive noise modeling for the observations of $\mathbf{z}_{ij}(k)$

$$\mathbf{y}_{ij}(k) = \mathbf{z}_{ij}(k) + \mathbf{v}_{ij}(k) \quad i \in \mathcal{V}_f, j \in \mathcal{N}_i^k, \quad (4)$$

where the noise $\mathbf{v}_{ij}(k)$ has zero mean and a covariance of $\mathbf{R}_{ij}$. It is assumed that observation noises are i.i.d. across all edges. We introduce a binary variable $\nu_{ij}(k)$ for all observations across time to represent their availability, i.e., $\nu_{ij}(k) = 1$ when $\mathbf{y}_{ij}(k)$ is available, otherwise $\nu_{ij}(k) = 0$. If observation losses are intermittent across time, we model $\nu_{ij}(k)$ as a Bernoulli process characterized by a unified λ, the probability of arrival.

III. Relative Kalman Filtering

In this section, we focus on the estimation of relative positions across time through a relative Kalman filter (RKF) as it exhibits robustness to intermittent losses [22]. With the observation model given by (4), the challenge is to model the relative dynamics. A straightforward way is to subtract the agents' dynamics (3) of neighboring agents [22], but this imposes high demands on communication in terms of delay and consistency, which can be impractical in case of observation losses. Alternatively, it is preferred to adopt a local approximation of the relative dynamics that does not require communication. Since we assume linear dynamic motions of the agents, we also assume their relative dynamics model is also linear. Given the knowledge of the leaders' dynamics,

various approximate linear models can be assumed e.g., constant velocity and constant acceleration. Here we present the constant acceleration model for generality but others can also be adopted under appropriate circumstances.

A. Relative State-space Model

For the constant acceleration model, an extended (relative) state vector $\mathbf{z}'_{ij} \in \mathbb{R}^{3D}$ is defined as

$$\mathbf{z}'_{ij}(k) = \text{vec}([\mathbf{z}_{ij}(k), \dot{\mathbf{z}}_{ij}(k), \ddot{\mathbf{z}}_{ij}(k)]^T), \tag{5}$$

where $\dot{\mathbf{z}}_{ij}(k)$ and $\ddot{\mathbf{z}}_{ij}(k)$ are the (relative) velocity and acceleration, respectively. Then the relative state-space model is given as

$$\begin{cases} \mathbf{y}_{ij}(k) = \mathbf{G}\mathbf{z}'_{ij}(k) + \mathbf{v}_{ij}(k) \\ \mathbf{z}'_{ij}(k+1) = \mathbf{F}\mathbf{z}'_{ij}(k) + \mathbf{w}_{ij}(k) \end{cases} \tag{6}$$

where in the observation model $\mathbf{G} = \mathbf{I}_D \otimes [1\ 0\ 0]$ and $\mathbf{v}_{ij}(k) \sim \boldsymbol{\mathcal{N}}(\mathbf{0}_D, \mathbf{R}_{ij})$ recollecting from (4). In the dynamic model,

$$\mathbf{F} = \mathbf{I}_D \otimes \begin{bmatrix} 1 & \Delta t & \frac{1}{2}\Delta t^2 \\ 0 & 1 & \Delta t \\ 0 & 0 & 1 \end{bmatrix}, \tag{7}$$

assuming no correlation across dimensions and $\mathbf{w}_{ij}(k) \sim \boldsymbol{\mathcal{N}}(\mathbf{0}, \mathbf{Q}_{ij})$ is the process noise, which is used to approximate the inaccuracy of the state transition model caused by assuming constant acceleration. The covariance matrix $\mathbf{Q}_{ij}$ shall have the structure of

$$\mathbf{Q}_{ij} = \sigma_w^2 \mathbf{I}_D \otimes \begin{bmatrix} \frac{\Delta t^4}{4} & \frac{\Delta t^3}{2} & \frac{\Delta t^2}{2} \\ \frac{\Delta t^3}{2} & \Delta t^2 & \Delta t \\ \frac{\Delta t^2}{2} & \Delta t & 1 \end{bmatrix}, \tag{8}$$

where σ_w^2 is the variance of acceleration uncertainty. This structure can be derived by projecting small deflections of acceleration in the state vector.

B. RKF under Observation Losses

Following the approach in a formation control framework proposed in [20], we have the following Relative Kalman Filter. For all $i \in \mathcal{V}_f, j \in \mathcal{N}_i$,

RKF prediction stage

$$\hat{\mathbf{z}}'_{ij}(k|k-1) = \mathbf{F}\hat{\mathbf{z}}'_{ij}(k-1|k-1) \tag{9a}$$

$$\boldsymbol{\Sigma}_{ij}(k|k-1) = \mathbf{F}\boldsymbol{\Sigma}_{ij}(k-1|k-1)\mathbf{F}^T + \mathbf{Q}_{ij} \tag{9b}$$

RKF correction stage

$$\mathbf{K}_{ij}(k) = \boldsymbol{\Sigma}_{ij}(k|k-1)\mathbf{G}^T(\mathbf{R}_{ij} + \mathbf{G}\boldsymbol{\Sigma}_{ij}(k|k-1)\mathbf{G}^T)^{-1} \tag{10a}$$

$$\hat{\mathbf{z}}'_{ij}(k|k) = \hat{\mathbf{z}}'_{ij}(k|k-1) + \nu_{ij}(k)\mathbf{K}_{ij}(k)(\mathbf{y}_{ij}(k) - \mathbf{G}\hat{\mathbf{z}}'_{ij}(k|k-1)) \tag{10b}$$

$$\boldsymbol{\Sigma}_{ij}(k|k) = (\mathbf{I}_{3D} - \nu_{ij}(k)\mathbf{K}_{ij}(k)\mathbf{G})\boldsymbol{\Sigma}_{ij}(k|k-1) \tag{10c}$$

where $\nu_{ij}(k)$ is the binary availability variable. The estimated relative positions can then be extracted by applying the matrix $\mathbf{G}$ again on the estimated state vector. Since the filter is built for every edge, it can be carried out in a distributed manner on each agent.

This method relies on intermittent observations to correct for the large variance accumulated by making predictions. When observations are unavailable for a longer time, i.e., under consecutive losses, the predictions can quickly deviate from the truth, as will be shown later in numerical examples. In these cases, alternative estimators that are independent of the dynamics of agents are needed, which will be shown in the next section.

IV. Relative Affine Localization

In this section, we focus on the estimation in a single time instance, but we broaden our view from a single relative position to all agents in the neighborhood. A local view of observation losses is whether a relative position w.r.t. some neighbors can be acquired. As such, for each agent $i \in \mathcal{V}_f$, we split the set of neighbors into $\mathcal{N}_i = (\mathcal{N}_i^k, \mathcal{N}_i^m)$ in which $\mathcal{N}_i^k$ contains the neighbors w.r.t. whom the relative position observations are known, and $\mathcal{N}_i^m$ contains the neighbors w.r.t. whom the observations are missing or unavailable. Then the cardinality $|\mathcal{N}_i^k|$ indicates the number of available observations for agent i. The goal is then to estimate $\mathbf{z}_{ij}$ for $j \in \mathcal{N}_i^m$ given $\mathbf{z}_{ij}$ for $j \in \mathcal{N}_i^k$. The split of the set of neighbors can be random or consecutive across time based on the nature of observation losses.

The proposed estimator can be considered as a relative localization method from the property of affine transformation and is called relative affine localization (RAL). We will now show that agents can locally determine the missing relative positions of some neighbors given at least D relative positions in the neighborhood. Recollect the nominal positions $\mathbf{p}_i$ that are prescribed and known and define relative nominal positions as $\mathbf{p}_{ij} = \mathbf{p}_i - \mathbf{p}_j$ for all $i \in \mathcal{V}$, and a matrix $\mathbf{P}_i = [\mathbf{p}_{i1}, ..., \mathbf{p}_{i|\mathcal{N}_i|}] \in \mathbb{R}^{|\mathcal{N}_i| \times D}$ that locally stores $\mathbf{p}_{ij}$ in the neighborhood. Similarly, a matrix that stores the relative positions in the neighborhood is $\mathbf{Z}_i = [\mathbf{z}_{i1}, ..., \mathbf{z}_{i|\mathcal{N}_i|}] \in \mathbb{R}^{|\mathcal{N}_i| \times D}$. To denote the missing observations, we define a local observation matrix $\boldsymbol{\Phi}_i(k) \in \mathbb{R}^{|\mathcal{N}_i^k| \times |\mathcal{N}_i|}$ that sieves the available relative positions in the neighborhood. It has the structure shown in Fig. 2 where $\mathbf{X}_i \in \mathbb{R}^{|\mathcal{N}_i^k| \times D}$ aggregates all the available relative positions.

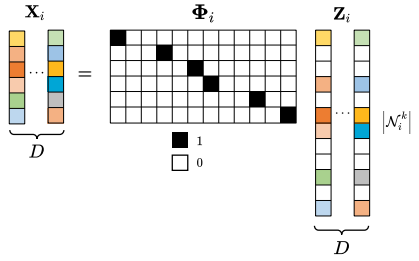

Fig. 2. Illustration of the selection matrix $\boldsymbol{\Phi}_i$

Theorem 1 (*Relative affine localization*)**.** Assume configuration $\mathbf{z}(k) \in \mathbb{R}^{DN}$ is in affine image $\mathcal{A}(\mathbf{p})$. For agent $i \in \mathcal{V}_f$,

given the split $\mathcal{N}_i = (\mathcal{N}_i^k, \mathcal{N}_i^m)$, the missing relative positions $\{\mathbf{z}_{ij}(k)\}_{j\in\mathcal{N}_i^m}$ can be locally and uniquely determined if and only if $\mathbf{H}_i(k) \triangleq \mathbf{\Phi}_i(k)\mathbf{P}_i$ is full column rank.

Proof. If configuration $\mathbf{z}(k) \in \mathbb{R}^{DN}$ is in affine image $\mathcal{A}(\mathbf{p})$, then by definition it holds that

$$\begin{aligned}\mathbf{z}_{ij}(k) &= \mathbf{z}_i(k) - \mathbf{z}_j(k)\\ &= \mathbf{\Theta}(k)\mathbf{p}_i + \mathbf{t}(k) - (\mathbf{\Theta}(k)\mathbf{p}_j + \mathbf{t}(k))\\ &= \mathbf{\Theta}(k)\mathbf{p}_{ij}\end{aligned} \tag{11}$$

for $i \in \mathcal{V}_f, j \in \mathcal{N}_i$. Then a local set of linear equations could be established as $\mathbf{Z}_i(k) = \mathbf{P}_i\mathbf{\Theta}(k)^T$. By applying the observation matrix $\mathbf{\Phi}_i(k)$ on both sides, we have

$$\mathbf{X}_i(k) = \mathbf{\Phi}_i(k)\mathbf{P}_i\mathbf{\Theta}(k)^T = \mathbf{H}_i(k)\mathbf{\Theta}(k)^T, \tag{12}$$

where $\mathbf{X}_i(k)$ stores $\mathbf{z}_{ij}(k) \in \{\mathbf{z}_{ij}(k)\}_{j\in\mathcal{N}_i^k}$.
(Sufficiency) If $\mathbf{H}_i(k)$ full column rank, then the global affine transformation matrix $\mathbf{\Theta}(k)$ can be locally and uniquely determined by

$$\mathbf{\Theta}_i(k)^T = (\mathbf{H}_i(k)^T\mathbf{H}_i(k))^{-1}\mathbf{H}_i(k)^T\mathbf{X}_i(k), \tag{13}$$

followed by the local determination of missing observation

$$\mathbf{z}_{ij}(k) = \mathbf{\Theta}_i(k)\mathbf{p}_{ij} \quad j \in \mathcal{N}_i^m. \tag{14}$$

(Necessity) If $\mathbf{H}_i(k)$ is not full-column rank, then there exists no left inverse of $\mathbf{H}_i(k)$ which indicates that unique and non-trivial local estimation for $\mathbf{\Theta}(k)$ does not exist. Then items in $\{\mathbf{z}_{ij}(k)\}_{j\in\mathcal{N}_i^m}$ cannot be uniquely determined. ■

The rank condition implies that $|\mathcal{N}_i^k| \geq D$ and enforces some geometry requirements on the observations. The split $\mathcal{N}_i = (\mathcal{N}_i^k, \mathcal{N}_i^m)$ that fulfills these conditions are called *geometrically feasible* for relative affine localization. Some examples are given in Fig. 3 to further explain this feasibility. Another intuitive understanding of geometrical feasibility for RAL is the minimum number of independent equations to solve for the parameters $\mathbf{\Theta}(k)$ in the underlying affine transformation.

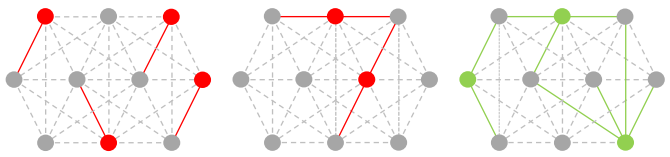

Fig. 3. Some examples of infeasible and feasible available observations to enable RAL in $\mathbb{R}^2$. Colored nodes represent agents of interest. (a) infeasible due to $|\mathcal{N}_i^k| < D$ locally. (b) infeasible due to collinear relative positions such that $\mathbf{H}_i$ is not full-rank. (c) feasible.

In practice, the assumption that $\mathbf{z}(k) \in \mathbb{R}^{DN}$ is in affine image $\mathcal{A}(\mathbf{p})$ rarely holds strictly due to insufficient formation convergence and observations noises. Based on (12) and noise model (4), the local linear equations can then be adapted as

$$\mathbf{Y}_i(k) = \mathbf{X}_i(k) + \mathbf{V}_i(k) = \mathbf{H}_i(k)\mathbf{\Theta}(k)^T + \mathbf{V}_i(k), \tag{15}$$

where $\mathbf{V}_i(k) = [\mathbf{v}_{i1}, ..., \mathbf{v}_{i|\mathcal{N}_i^k|}]^T$ in which $\mathbf{v}_{ij} \in \{\mathbf{v}_{ij}\}_{j\in\mathcal{N}_i^k}$ is the observation noise matrix for known relative positions. $\mathbf{\Theta}(k)$ can be estimated by the formulation of

$$\hat{\mathbf{\Theta}}_i(k) = \underset{\mathbf{\Theta}(k)}{\arg\min} \quad \left\|\mathbf{H}_i(k)\mathbf{\Theta}(k)^T - \mathbf{Y}_i(k)\right\|_F^2. \tag{16}$$

Next, the missing relative positions can be estimated by

$$\hat{\mathbf{z}}_{ij}^{\text{ral}}(k) = \hat{\mathbf{\Theta}}_i(k)\mathbf{p}_{ij}, \quad j \in \mathcal{N}_i^m. \tag{17}$$

On another note, if the affine transformations are limited to a few special cases such as scaling, rotation or similarity transform. The transformation matrix $\mathbf{\Theta}_i(k)$ will also have special structures with which we can levy constraints on the formulation (16) including diagonality and orthonormality constraints. This will limit the solution space and result in better estimates.

RAL is a very low-cost estimator because it uses only geometry information from the neighborhood and no additional sensor data are required. Also, this is a linear estimator that adds little stress to the onboard computers. If very few observations are missing in the neighborhood, the estimation can be of high accuracy. However, the quality of RAL estimates will degrade until the system has sufficiently converged to equilibrium as the premise for RAL that $\mathbf{z}(k)$ is in affine image $\mathcal{A}(\mathbf{p})$ is violated off-equilibrium. This would typically lead to a slower convergence and raise some challenges in the fusion as agents also need to locally determine the quality of RAL estimates.

V. Adaptive Fusion of RAL with Kalman Filtering

In the previous sections, we discussed the relative Kalman filter and the geometrically inferred RAL, which can be considered two sources of estimates that exhibit different levels of robustness for different types of losses. For instance, RAL is not very robust to very heavy losses, e.g., with very small λ in the intermittent cases, due to its geometrical feasibility requirement. On the other hand, RKF is not robust against consecutive observation losses since errors accumulate quickly without the correction of observation. In this section, we aim to combine these two types of estimators and propose an improved solution in both intermittent and consecutive loss settings.

A. Switching Observation Models

The fusion is done by treating RAL estimates as alternative observations when real observations are missing. Then in the RKF framework, there is a switching observation model for every relative position. Note that switching observations does not mean every missing relative position can be restored by RAL due to its geometrical feasibility requirements. But improvements in the performance can still be expected from the extra percentage of observations from RAL. Assuming the system has sufficiently converged, we can model the RAL observation as

$$\hat{\mathbf{z}}_{ij}^{\text{ral}}(k) = \mathbf{z}_{ij}(k) + \tilde{\mathbf{v}}_{ij}(k), \tag{18}$$

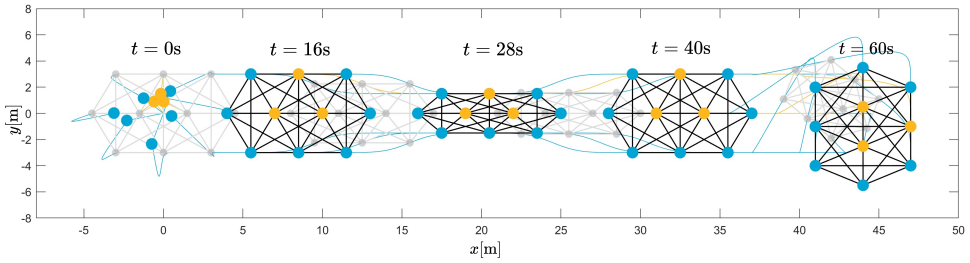

Fig. 4. The formation maneuver pattern in our work. The colored nodes denote the true positions of agents, and the translucent (light gray) nodes represent the target positions at other times.

where $\tilde{\mathbf{v}}_{ij}(k)$ is the equivalent noise of RAL estimates and has zero mean. This is because no bias is introduced in the estimations of $\boldsymbol{\Theta}(k)$ and $\hat{\mathbf{z}}_{ij}^{\text{ral}}(k)$ as they are strictly linear operations on the unbiased observations $\mathbf{y}_{ij}$. The covariance of this noise is closely related to the covariance of the estimates and is denoted by $\tilde{\mathbf{R}}_{ij}$.

B. Adaptive Penalty for Improved Convergence

It is discussed in the previous sections that RAL estimates before formation convergence are subject to large errors, thus a hard fusion of RAL estimates will also lead to larger errors and slow convergence. To modulate the Kalman filter such that it relies less on the RAL observations prior to convergence, we can penalize the covariance for RAL observations with large values. In this way, the Kalman filter will put less weight on the RAL observation. But it is also necessary to ensure that RAL observations are effective with sufficient formation convergence. As such, we propose the following adaptive penalty

$$\tilde{\mathbf{R}}_{ij}^{\text{mod}}(k) = \tilde{\mathbf{R}}_{ij} + \epsilon_i(k)\mathbf{I}_D \tag{19}$$

for $i \in \mathcal{V}_f$, where $\epsilon_i(k)$ is designed as

$$\epsilon_i(k) = \frac{1}{|\mathcal{N}_i|} \sum_{j \in \mathcal{N}_i} \left\| \hat{\boldsymbol{\Theta}}_i(k) - \hat{\boldsymbol{\Theta}}_j(k) \right\|_F^2 . \tag{20}$$

This function serves as a convergence indicator and mimics the tracking error based on the fact that local estimates of the affine transformation matrix should reach a consensus if affine formation is perfectly achieved. As such, when tracking error is hard to locally compute since the target positions are unknown to the followers, this indicator function is a good substitute with some extra communication cost.

As can be seen from (19), an additional term is added to penalize $\tilde{\mathbf{R}}_{ij}$. When the system is insufficiently converged, large $\epsilon_i(k)$ will make the penalty dominating and when the system is converged, small $\epsilon_i(k)$ will result in negligible influence on the structure of $\tilde{\mathbf{R}}_{ij}$. Now we conclude the switching observation models as

$$\tilde{\mathbf{y}}_{ij}(k) = \begin{cases} \hat{\mathbf{z}}_{ij}^{\text{ral}}(k), \text{with } \tilde{\mathbf{R}}_{ij}^{\text{mod}}(k), & \text{if } j \in \mathcal{N}_i^m \\ \mathbf{y}_{ij}(k), \text{with } \mathbf{R}_{ij}, & \text{if } j \in \mathcal{N}_i^k \end{cases} , \tag{21}$$

if there exist RAL estimates. Then the same procedures in RKF can be conducted with a replacement of $\mathbf{y}_{ij}(k)$ by $\tilde{\mathbf{y}}_{ij}(k)$ in the correction stage. This solution of adaptive fusion is named geometry-aware RKF (GA-RKF) for future reference.

VI. Simulations

Our work adopts a maneuvering pattern in $\mathbb{R}^2$ shown in Fig. 4 with the same nominal formation shown in Fig. 1. The graph has $N = 10$ nodes and $M = 30$ undirected edges. The initial positions of the agents are randomly drawn from a normal distribution $\boldsymbol{\mathcal{N}}(\mathbf{0}_D, \mathbf{P}_0)$. For this discrete-time control system, we choose 1kHz as the control frequency i.e., $\Delta t = 1$ms interval between successive control inputs and a simulation duration of 60s. The noise for the observations is chosen to be Gaussian with a covariance $\mathbf{R}_{ij} = 0.01\mathbf{I}$. The control law is taken as the one with time-varying leaders in Table I. The evaluation metric that we use in this paper is the tracking error which is defined as

$$\delta(k) = \frac{1}{D|\mathcal{V}_f|} \sum_{i \in \mathcal{V}_f} \|\mathbf{z}_i(k) - \mathbf{z}_i^*(k)\|_2 . \tag{22}$$

Next, we will show the performance improvements of the proposed methods under both intermittent and consecutive losses.

A. Intermittent Observation Losses

Recollect that the intermittent observations are modeled by a Bernoulli process with λ being the probability of availability.

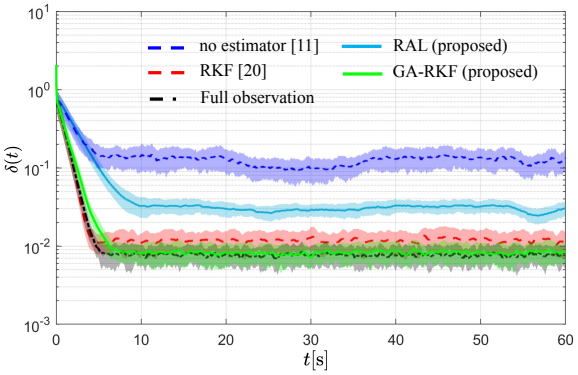

Fig. 5. Convergence by tracking error of the proposed solutions under 50% intermittent loss. The solid lines are the mean of 50 Monte Carlo experiments with random initialization and the translucent strips are the 1 standard deviation region.

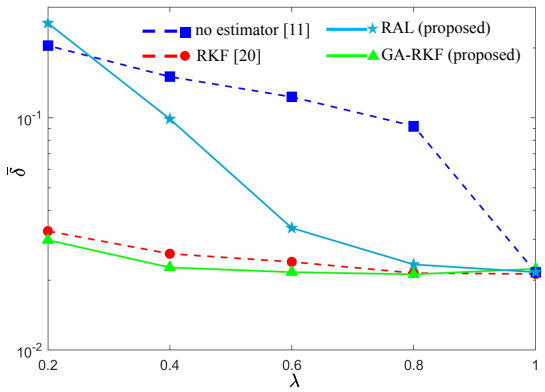

Fig. 6. Average tracking errors under different Bernoulli probability λ. The simulations are also averaged over 10 experiments.

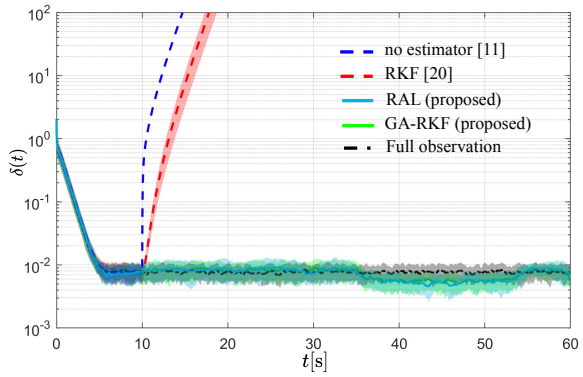

Fig. 8. Convergence by tracking error with consecutive observation losses caused by offline agents.

Fig. 5 shows the convergence across time in tracking error with $\lambda = 0.5$. The black dashed line represents the full observation case which can be considered an experimental error bound. Solutions closer to this line are preferred. The "no estimator" case is the default setup for the controller proposed in [11] in case of observation losses, which induces high error as observed in Fig. 5. If using only the estimation from geometry (RAL) the error is suppressed but still not close to the bound, and the convergence is slower. With RKF implemented, the convergence speed is guaranteed and the error is very low. Our proposed fusion solution GA-RKF exhibits close-to-bound performance with an accelerated formation convergence compared to the proposed RAL algorithm.

Similar conclusions can also be made with a spectrum of probability λ as shown in Fig. 6, where $\bar{\delta}$ is the averaged tracking error over all 60 seconds. $\lambda = 1$ is equivalent to the "Full observation" case in Fig. 5. Generally, the average tracking errors increase as λ decreases as a general trade-off of losing more observations. In the case of no estimators, the error is boosted even with a small percentage of observation losses. RAL shows robustness to slight losses, e.g., when $\lambda = 0.8$, but not to heavy losses as there is less chance to engage RAL estimation due to geometric feasibility issues. RKF shows strong resilience to heavy intermittent losses, e.g., when $\lambda = 0.2$. The fusion method GA-RKF further improves the performance compared to RKF.

B. Consecutive Observation Losses

We now examine their robustness in a consecutive or permanent loss setup. To motivate consecutive observation losses, we present a scenario in which one or more followers are disconnected from the formation and thus the associated observations are permanently missing. This occurs in practice when agents are out of service due to e.g., maintenance, scheduling, etc. and we still expect the rest of the agents to maintain the original formation. One instance of this scenario is shown in Fig. 7. In this case, the underlying graph is fundamentally changed to one that may be unstabilizable. As such, to prevent a diverging formation, constant estimations shall be performed regarding the missing observations as if a substitute virtual node is still running with the system.

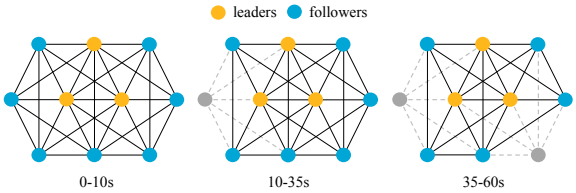

Fig. 7. The setup for consecutive observation losses, where 2 followers are offline successively in operation.

The performance of the proposed solutions in this setup can be seen in Fig. 8, where the two clear diverging curves are "no estimator" and RKF. For the "no estimator" case, the previous edge stress is no longer stabilizing the new graph. For the RKF case, the system is diverging because no observations at all provide corrections for the Kalman filter and the dynamics model will be soon too outdated to give satisfactory estimates. However, since two missing agents do not cause heavy edge losses in general, RAL and the fusion solutions perform well and the system remains almost unaffected. If there are additional consecutive node/edge losses, their performance is also expected to decline.

VII. Conclusions

In this work, we propose an adaptive fusion estimation for affine formation control framework under observation losses. Instead of using additional sensors, an alternative source of information is extracted from the geometry of affine formations which is then adaptively combined with the conventional Kalman filtering. The proposed GA-RKF exhibits stronger robustness to intermittent losses under low availability of observation, and also to consecutive losses in cases of offline agents compared to the conventional distributed Kalman filtering (RKF) or relative affine localization (RAL) alone. In our future work, we aim to report rigorous theoretical bounds such as posterior Cramér-Rao bounds for the given data model, to investigate the optimality of the proposed solutions.

REFERENCES

[1] F. Yang, S. Liu, and F. Liu, "Cooperative transport strategy for formation control of multiple mobile robots," in *Journal of Zhejiang University SCIENCE C*, vol. 11, pp. 931–938, 2010.

[2] L. Chen, H. Hopman, and R. R. Negenborn, "Distributed model predictive control for cooperative floating object transport with multi-vessel systems," in *Ocean Engineering*, vol. 191, pp. 106515, 2019.

[3] D. Becker, M. D. Lachmann, S. T. Seidel, et al, "Space-borne Bose–Einstein condensation for precision interferometry," in *Nature*, vol. 562, pp. 391–395, 2018.

[4] G. Liu and S. Zhang, "A survey on formation control of small satellites," in *Proceedings of the IEEE*, vol. 106, pp. 440–457, 2018.

[5] B. Das, B. Subudhi, and B.B., Pati, "Cooperative formation control of autonomous underwater vehicles: An overview," in *International Journal of Automation and Computing*, vol. 13, pp. 199–225, 2016.

[6] Z. Wang, Z. Zhu, Z. Wei, X. Huang and B. Yin, "Research on Formation Control of Multiple Autonomous Underwater Vehicle Systems with Limited Communication," in *2017 International Conference on Computer Systems, Electronics and Control (ICCSEC)*, pp. 343-346, 2017.

[7] Z. Li, Z. Duan, G. Chen and L. Huang, "Consensus of Multiagent Systems and Synchronization of Complex Networks: A Unified Viewpoint," in *IEEE Transactions on Circuits and Systems I: Regular Papers*, vol. 57, no. 1, pp. 213-224, 2010.

[8] R. Suttner, and Z. Sun, "Formation Shape Control Based on Distance Measurements Using Lie Bracket Approximations," in *SIAM Journal on Control and Optimization*, vol. 56, pp. 4405-4433, 2018.

[9] S. Zhao and D. Zelazo, "Translational and Scaling Formation Maneuver Control via a Bearing-Based Approach," in *IEEE Transactions on Control of Network Systems*, vol. 4, pp. 429-438, 2017.

[10] Z. Lin, L. Wang, Z. Chen, M. Fu and Z. Han, "Necessary and Sufficient Graphical Conditions for Affine Formation Control," in *IEEE Transactions on Automatic Control*, vol. 61, pp. 2877-2891, 2016.

[11] S. Zhao, "Affine Formation Maneuver Control of Multiagent Systems," in *IEEE Transactions on Automatic Control*, vol. 63, pp. 4140-4155, 2018.

[12] B. Khaleghi, A. Khamis, F. O. Karray, and S. N. Razavi, "Multisensor data fusion: A review of the state-of-the-art," in *Information Fusion*, vol. 14, no. 1, pp. 28–44, Jan. 2013.

[13] D. Y. Kim, J. H. Yoon, Y. H. Kim and V. Shin, "Distributed information fusion filter with intermittent observations," in *13th International Conference on Information Fusion (FUSION)*, pp. 1-7, 2010.

[14] Y. Luo, Y. Zhu, X. Shen and E. Song, "Distributed Kalman filtering fusion with packet loss or intermittent communications from local estimators to fusion center," in *Journal of Systems Science & Complexity*, vol. 25, pp. 463-485, 2012.

[15] Y. Liang, Y. Li, S. Chen, G. Qi, and A. Sheng, "Event-triggered Kalman consensus filter for sensor networks with intermittent observations," in *International Journal of Adaptive Control and Signal Processing*, vol. 35, pp. 8, 2021.

[16] J. Xu, X. Wu and Y. Tang, "Optimal Linear Exponential Quadratic Gaussian Estimation With Intermittent Observations," in *IEEE Control Systems Letters*, vol. 3, pp. 936-941, 2019.

[17] Q. Zhang, G. Yin and L. Wang, "A Deep Filtering Approach for Control of Partially Observed Systems," in *IEEE Control Systems Letters*, vol. 5, pp. 1189-1194, 2021.

[18] Y. Wu ,J. Zhang ,Y. Ge, Z. Sheng, and Y. Fang, "A Dropout Compensation ILC Method for Formation Tracking of Heterogeneous Multi-Agent Systems with Loss of Multiple Communication Packets," in *Appled Sciences*, vol. 10, 4752, 2020.

[19] L. Sedghi, J. John, M. Noor-A-Rahim, and D. Pesch, "Formation Control of Automated Guided Vehicles in the Presence of Packet Loss," in *Sensors*, vol. 22, 3552, 2022.

[20] J. Lee, S. Y. Park, and D. E. Kang, "Relative Navigation with Intermittent Laser-based Measurement for Spacecraft Formation Flying," in *Journal of Astronomy and Space Sciences*, vol. 35, no. 3, pp. 163–173, Sep. 2018.

[21] S. Chen, D. Yin, and Y. Niu, "A Survey of Robot Swarms Relative Localization Method," in *Sensors*, vol. 22, no. 12, 2022.

[22] M. van der Marel, and R. T. Rajan, "Distributed Kalman Filters for Relative Formation Control of Multi-Agent Systems," in *2022 30th European Signal Processing Conference (EUSIPCO)*, pp. 1422-1426, 2022.